

# ULTRASHORT AND COHERENT RADIATION FOR PUMP-PROBE EXPERIMENTS AT THE DELTA STORAGE RING\*

M. Huck<sup>†</sup>, S. Hilbrich, M. Höner, H. Huck, S. Khan, C. Mai,

A. Meyer auf der Heide, R. Molo, H. Rast, A. Schick, P. Ungelenk,

Center for Synchrotron Radiation (DELTA), TU Dortmund University, Dortmund, Germany

## Abstract

A light source facility employing the coherent harmonic generation (CHG) principle is being commissioned and operated since 2011 at DELTA, a 1.5-GeV electron storage ring at the TU Dortmund University, with the purpose of providing ultrashort coherent VUV radiation for time-resolved experiments. CHG is based on the interaction of ultrashort laser pulses with electrons in an undulator to generate coherent harmonics of the laser wavelength. Different methods have been used to optimize, detect and characterize the CHG radiation. One example is the study of transverse and longitudinal coherence properties in double-slit and Michelson experiments. Moreover, final steps towards performing pump-probe experiments to study ultrafast magnetic phenomena have been taken.

## INTRODUCTION

DELTA is a 1.5-GeV synchrotron radiation light source operated by the Center for Synchrotron Radiation at the TU Dortmund University. The source for ultrashort VUV pulses (Fig. 1) based on the coherent harmonic generation (CHG) principle [1–4] is in operation at DELTA since 2011 [5–7].

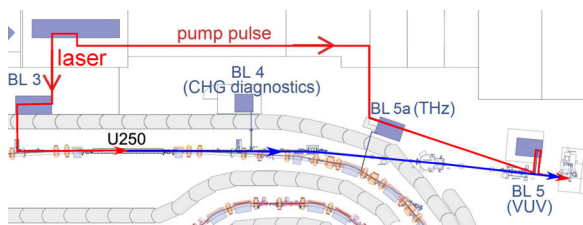


Figure 1: The layout of the CHG facility at DELTA.

A Ti:sapphire femtosecond laser system is used for seeding, either with its standard wavelength of 800 nm (796 nm, to be more precise) or with its second harmonic, generated in a BBO crystal. The 800 nm laser pulses are focused by a lens telescope at beamline 3 (BL 3) into the undulator (U250). For seeding with 400 nm, a mirror telescope is used to minimize the effects of group-delay dispersion. The undulator consists of three parts, namely modulator, dispersive chicane and radiator (in an optical-klystron configuration, Fig. 2) with separate power supplies. In the modulator, the electric field of the laser pulses modulates the energy of the electrons periodically in a small slice of the bunch ( $10^{-3}$  of its length). The dispersive chicane causes the modulated electrons to travel on trajectories of different length and

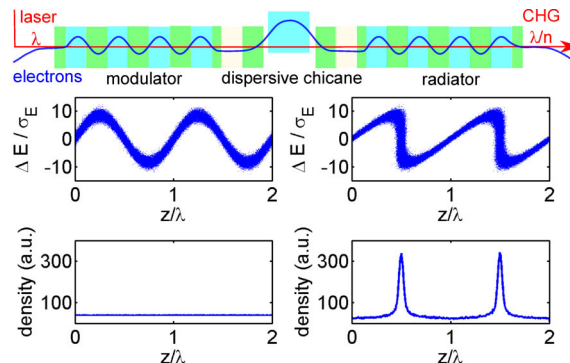


Figure 2: Optical-klystron configuration and CHG principle. The laser-induced energy modulation in the modulator (left) and the density modulation after passing the chicane (right) are shown in longitudinal phase space.

hence to form microbunches, which radiate coherently in the radiator at a harmonic of the seed wavelength. Finally, the CHG radiation is sent either via BL 4 to a diagnostics hutch for optimization and characterization, or to a VUV beamline (BL 5) [10] for detection and application in user experiments. The main parameters are shown in Table 1.

Due to path length differences acquired by the off-energy electrons within the bending magnets downstream of the undulator, a sub-millimeter gap in the longitudinal density profile is created. This causes the emission of coherent THz radiation, which is extracted via a dedicated beamline (BL 5a), equipped with an InSb-bolometer, a YBCO detector and an FT-IR spectrometer, and can be used as a diagnostics tool for the laser-electron overlap and accelerator studies [9] as well as for time-resolved far-infrared spectroscopy. A dedicated beamline has been constructed to guide a fraction of the laser pulses to the experimental stations at BL 5 and BL 5a for the purpose of pump-probe experiments.

Table 1: Specifications of the CHG facility at DELTA

bunch length (FWHM)	~ 100 ps
single-bunch current / charge	up to 20 mA / 7.7 nC
revolution frequency	2.6 MHz
number of modulator periods	7
number of radiator periods	7
length of undulator periods	250 mm
K value of modulator / radiator	0 - 11
$r_{56}$ value of chicane	0 - 130 $\mu$ m
laser pulse energy @400 nm	up to 2.6 mJ @ 1 kHz
laser pulse energy @800 nm	up to 8 mJ @ 1 kHz
pulse duration (FWHM)	~ 40 fs

\* Work supported by DFG, BMBF, and by the Federal State NRW.

<sup>†</sup> Maryam.Huck@tu-dortmund.de

## GENERAL RESULTS

In early measurements in 2011, the quadratic dependence of the CHG and THz radiation intensity on the bunch current was verified [5]. After optimization of the chicane in early 2013, the photoelectron yield at BL 5 showed an intensity ratio between short CHG pulses and spontaneous undulator radiation from the whole bunch of about 600 at 200 nm and 150 at 133 nm (second and third harmonics of 400 nm) at 1% bandwidth [7, 8]. Furthermore, spectra of coherent THz pulses were measured, turn-by-turn THz pulses were detected up to the 11<sup>th</sup> turn using fast bolometers, and narrowband THz radiation was produced by modulating the intensity of the seed-laser pulses using a Michelson interferometer [11–13].

## STUDY OF CHG SPECTRA

The spectral properties of CHG radiation below 200 nm were studied by photoemission under variation of the plane-grating monochromator of BL 5. For longer wavelengths, a CCD spectrometer and a Czerny-Turner-type monochromator equipped with an avalanche photodiode were used. Assuming a pulse duration of 100 fs, the width of the nearly Gaussian CHG spectra was usually close to the Fourier limit [7]. However, when deviating from optimized laser and chicane parameters, the spectral shape changes drastically, reflecting the longitudinal variation of the seed-pulse intensity. For example, increasing the chicane strength leads to an optimum bunching factor (given by constant  $r_{56} \cdot \Delta E$ ) for electrons with lower energy modulation  $\Delta E$  on the slopes of the seed pulse while overbunching the central part. This results in a coherent double pulse, the spectrum of which contains interference fringes. The time between the two pulses should increase with  $r_{56}$  while the spectral separation of the fringes should decrease. This tendency is clearly observed in the example of Fig. 3, the second harmonic of 800 nm (corresponding to a frequency around 750 THz) with  $r_{56} =$  values of 20, 53, and 102  $\mu\text{m}$ , but the spectra contain additional unexpected features such as the suppression of the central peak. Further measurements have shown that a slight misalignment of the Ti:sapphire laser compressor, which leads to chirped pulses, can produce such features. Additional measurements and simulations are required to arrive at a quantitative understanding of the rich spectral structure observed in CHG radiation under various conditions.

## COHERENCE OF CHG PULSES

The coherence properties of the CHG pulses were studied employing interference experiments. The interference patterns were recorded by using a fast-gated intensified CCD camera [14]. A bandpass filter was placed right before the camera to eliminate the seed laser light, reducing the bandwidth of the spontaneous radiation, but not affecting the bandwidth of CHG, which is about 1%. A double-slit interference pattern of CHG radiation with a visibility of  $V = 0.9$  is shown in Fig. 4, recorded at a distance of  $L = 1.3$  m from the slits. The visibility of interference fringes

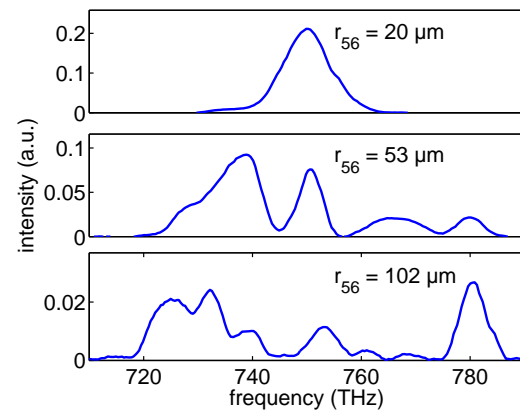


Figure 3: CHG spectra around 400 nm (750 THz), the second harmonic of the seed wavelength, under variation of the chicane strength.

$V = (I_{\max} - I_{\min}) / (I_{\max} + I_{\min})$  equals the coherence degree if both slits are equally illuminated. In this example, the slit width was  $w = 50 \mu\text{m}$  and the slit separation  $d = 200 \mu\text{m}$ . The fit function is given by

$$I(x) = S(x) \left[ 1 + V(x) \cos \left( \frac{2\pi d}{L\lambda} x \right) \right], \quad (1)$$

with  $S(x) = I_1(x) + I_2(x)$ , the sum of the intensity distribution of the single-slit diffraction in the near field ( $I_{1,2}(x) = (\sin(u_{1,2})/u_{1,2})^2$  and  $u_{1,2} = \pi w(x \pm d/2)/(L\lambda)$ ).

Furthermore, the transverse coherence length defined by  $r_c = \int_0^\infty |V(d)/V_{\max}|^2 dd$  was determined by conducting double-slit experiments with different slit separation  $d$ . The coherence function of 400- and 200-nm CHG radiation (seed wavelength 800 nm) with a coherence length of about  $r_c = 1.5$  mm and 0.8 mm, respectively, is shown in Fig. 4, measured with a slit width of 100  $\mu\text{m}$  at a distance of 10 m from the undulator.

The transverse coherence properties are also investigated in an ongoing collaboration with the University of Siegen, analyzing speckle patterns generated by single CHG pulses which are scattered from a thin organic film [15].

The temporal coherence length was studied both with a Michelson interferometer and by introducing two non-coated

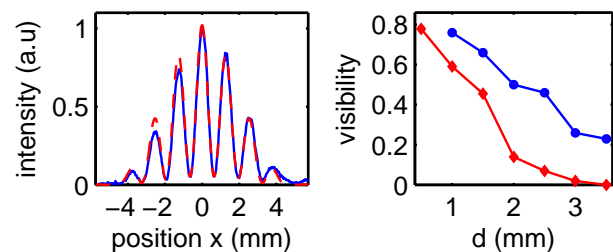


Figure 4: Left: Measured interference pattern of 200-nm CHG radiation (blue) and its fit (red dashed line). Right: The transverse coherence (visibility) as function of slit separation  $d$ , measured with 400-nm (blue) and 200-nm (red) CHG radiation at a distance of about 10 meters from the undulator.

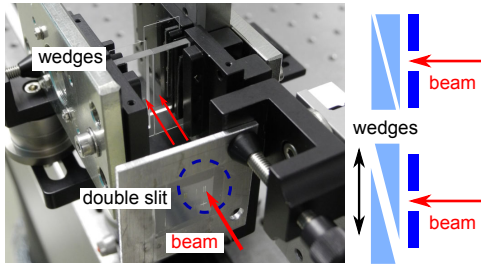


Figure 5: Photo and sketch of the double-slit setup followed by fused-silica wedges.

fused silica wedges in front of each slit of the double-slit setup (Fig. 5). The vertical position of one of the wedges was varied ( $\Delta y$ ), using a micrometer stage. Thus, the optical path length of one beam with respect to the other was varied by  $\Delta z = (n_f - 1)\Delta y \tan \theta$  (wedge angle  $\theta = 4^\circ$ , refractive index  $n_f = 1.55$  at 200 nm). Figure 6(a) shows the interference pattern using slits of width  $w = 100 \mu\text{m}$  and separation  $d = 0.5 \text{ mm}$ , and the 2D FFT of the interference pattern, and Fig. 6(b) shows the normalized coherence degree versus the delay. In Fourier space, the amplitude  $\tilde{I}$  at the side/central peak corresponds to the cross-/auto-correlation of two beams (XC/AC). The coherence degree  $\gamma(\tau)$  and coherence time  $\tau_c$  can be derived by [16]

$$\gamma(\tau) = \frac{\tilde{I}_{XC}}{\tilde{I}_{AC}}, \quad \tau_c = \int_{-\infty}^{\infty} \left| \frac{\gamma(\tau)}{\gamma(0)} \right|^2 d\tau. \quad (2)$$

Preliminary results from both methods (Michelson and wedges) yield a coherence time of  $\sim 34 \text{ fs}$ , which is somewhat shorter than the theoretical value for a Gaussian pulse  $\tau_c = 0.66\lambda_0^2/\Delta\lambda$  expected from spectral measurements. The double-slit dimensions and the chirp occurring in the wedges and in the Michelson beamsplitter are possible reasons for this discrepancy.

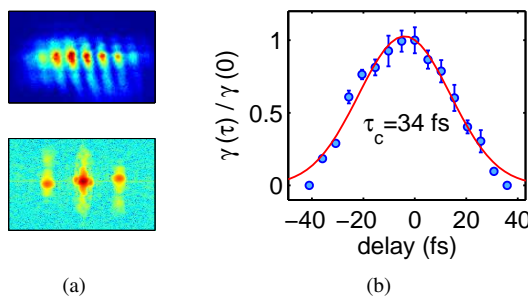


Figure 6: a) Interference pattern of 200-nm CHG radiation 1.3 m downstream of the double slit at equal wedge thickness (top) and its 2D Fourier transform (bottom). b) Measured coherence function (blue circles) and Gaussian fit (red curve).

## PUMP-PROBE EXPERIMENTS

CHG radiation up to the 7<sup>th</sup> harmonic (10.8 eV) of the 800-nm seed laser and 5<sup>th</sup> harmonic (15.5 eV) of the 400-nm seed was detected at BL 5 using photoelectron spectroscopy. A first proof-of-principle experiment was realized by detecting the surface state of a Cu(111) sample, using 9.35-eV

CHG radiation [22]. After detecting CHG radiation at BL 5, focusing the pump pulses on the sample and achieving zero delay between the pump- and seed-laser pulses, the preparations for pump-probe photoemission experiments are nearly completed. The first experiment will be performed on a Co/Cu magnetic system using the linear magnetic dichroism effect [17] in order to study the demagnetization dynamics in this thin-film system.

## SUMMARY AND OUTLOOK

The coherence properties of CHG pulses were determined by interferometric experiments. Most preparations for laser-pump CHG-probe experiments are completed. User experiments with CHG radiation are planned with a hybrid fill of the storage ring, i.e. a high-current single bunch in the gap of a 3/4 multibunch pattern. In order to improve the beam lifetime, an RF phase modulation is routinely applied in multibunch mode. It has been shown that the modulation does not impair CHG in hybrid mode, since the single bunch can be stabilized by a longitudinal feedback system [18] and/or the laser can be synchronized to the induced quadrupole oscillation, hitting the bunch when the electron density is largest. Initially, CHG user experiments will be performed with a photon energy of 9.3 eV, while the intermediate goal is a photon energy of 23 eV. Even shorter wavelengths can be generated by a planned upgrade of the DELTA short-pulse facility based on the echo-enabled harmonic generation (EEHG) technique [19]. This upgrade requires additional chicanes and undulators, as well as major modifications of the magnet lattice and vacuum chamber of the storage ring, in order to provide a long enough straight section without dispersive dipoles. The laser-induced energy modulation can also be exploited to generate ultrashort pulses of incoherent radiation at arbitrary wavelengths (femtosing) [20]. The proposed storage ring modification (Fig. 7) will provide enough free space for both an EEHG setup and a femtosing undulator [21].

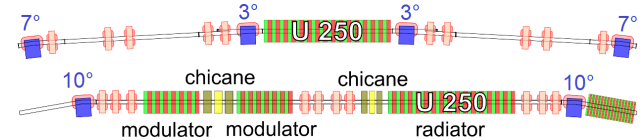


Figure 7: Sketch of the northern straight section at DELTA: present (top) and planned for EEHG (bottom). Blue numbers refer to bending magnet angles.

## ACKNOWLEDGMENTS

We are pleased to thank our colleagues at DELTA and other institutes, particularly FZJ/Jülich, HZB/Berlin, DESY/Hamburg and KIT/Karlsruhe, for their continuous support and advice. The financial support provided by DFG (INST 212/236-1 FUGG), BMBF (05K13PEC) and NRW Forschungsschule is gratefully acknowledged.

## REFERENCES

- [1] R. Coisson et al., Phys. of Quant. Electron. 9, 939 (1982).
- [2] B. Girard et al., PRL 53, 2405 (1984).
- [3] E. Allaria et al., PRL 100, 174801 (2008).
- [4] M. Labat et al., PRL 101, 164803 (2008).
- [5] S. Khan et al., Sync. Rad. News 24, 18 (2011).
- [6] H. Huck et al., Proc. FEL 2012, Nara, 12.
- [7] S. Khan et al., Sync. Rad. News 26, 25 (2013).
- [8] M. Huck et al., Proc. IPAC 2013, Shanghai, 2939.
- [9] P. Ungelenk et al., Proc. IPAC 2013, Shanghai, 94.
- [10] L. Plucinski et al., J. Elspec., 181, 215 (2010).
- [11] C. Evain et al., PRST-AB 13, 090703 (2010).
- [12] S. Bielawski et al., Nature Physics 4, 390 (2008).
- [13] P. Ungelenk et al., WEPRO002, this conference.
- [14] The camera was generously provided by B. Schmidt and S. Wunderlich, DESY, Hamburg.
- [15] C. Gutt et al., PRL 108, 024801 (2012).
- [16] A. Singer et al., Optics Express. 20, 16, 17480 (2012).
- [17] D. Venus et al., PRB 55, 2594 (1997).
- [18] M. Höner et al., THPME104, this conference.
- [19] G. Stupakov, Phys. Rev. Lett. 102, 074801 (2009).
- [20] A. A. Zholents et al., Phys. Rev. Lett. 76, 912 (1996).
- [21] R. Molo et al., FEL 2013, New York, 594.
- [22] S. Döring et al., 9<sup>th</sup> DELTA User Meeting & Annual Report (2013).